

Self-Organization in a Granular Medium by Internal Avalanches

S. S. Manna

Satyendra Nath Bose National Centre for Basic Sciences, Block-JD, Sector-III, Salt Lake, Calcutta-700098, India

Internal avalanches of grain displacements can be created inside a granular material kept in a bin in two ways: (i) By removing a randomly selected grain at the bottom of the bin (ii) By breaking a stable arch of grains clogging a hole at the bottom of the bin. Repeated generations of such avalanches lead the system to a steady state. The question asked, is this state a critical state as that in Self-Organized Criticality? We review here some of the recent studies on this problem using cellular automata as well as hard disc models.

PACS number(s): 05.70.Jk Critical Point Phenomena - 74.80.Bj Granular, melt-textured, and amorphous superconductors; powders

1. Introduction

A granular material is a collection of a large number of solid grains, such as sand, seeds, sugar, salt, stone chips etc. [1,2]. A granular material can be poured like a liquid into a container and also can form a pile against gravity like a solid. For this reason, a granular material is widely regarded as the fourth state of matter.

Use of granular materials is quite extensive in the industry and in the daily lives. Powders are routinely used in the food and pharmaceutical industries. Large quantities of sand and stone chips are used for the construction of highways and barrages. Food materials like flour, cereals, carbon, salts are transported, processed and stored. Apart from these the geological processes like landslides and snow avalanches on mountains involve granular materials. In spite of so many applications, flow of grains in granular materials and packing phenomena are not well understood from a fundamental viewpoint though the study of granular materials goes back to few centuries [3].

Recently a new idea was proposed by Bak, Tang and Wiesenfeld (BTW) to explain the formation of avalanches on the surface of a sandpile and is called 'Self-Organized Criticality' (SOC) [4]. Self-Organized Criticality is the emergence of long-ranged spatio-temporal correlations in non-equilibrium steady states of slowly driven systems without fine tuning of any control parameter. It says that there are certain class of systems in nature which become critical under their own dynamical evolutions. An external agent triggers into a system a transport process of some physical entity, say mass. The transport process is made of a large number of microscopic relaxation events. This cascade of events together is called an avalanche. After large number of avalanches, the system arrives at a *critical state*, when the avalanches extend over all length and time scales [4-6].

BTW observed that a typical sandpile satisfies all the criteria of SOC. Consider a sandpile formed on a fixed horizontal base, with an arbitrary initial distribution of sand. The pile is grown by adding repeatedly a few grains of sand at a time. After a long time the sandpile takes

a fixed conical shape and the system is said to reach the steady state. Addition of each sand grain results some activity on the surface of the pile: an avalanche of sand mass followed, which propagates on the surface of the sandpile. These avalanches are of many different sizes and BTW expected that they should have a power law distribution in the steady state.

Laboratory experiments on sand piles, however, have not been fully successful yet to show unambiguously the existence of SOC in sandpile systems. In the first experiment, the granular material was kept in a semicircular drum which was slowly rotated about the horizontal axis, thus slowly tilting the free surface of the pile [7]. Grains fell vertically downward and were allowed to pass through the plates of a capacitor. Power spectrum analysis of the time series for the fluctuating capacitance however showed a broad peak, contrary to the expectation of a power law decay, from the ideas of SOC [7].

In a second experiment, sand mass was slowly dropped on to a horizontal circular disc, to form a conical pile in the steady state [8]. On further sand addition, sand avalanches were created on the surface of the pile, and the outflow statistics was observed. Size of the avalanche was measured by the amount of sand mass that dropped out of the system. It was observed that the avalanche size distribution obeys a scaling behaviour for small sizes of the base. For large base, however the scaling did not work very well. It was suggested that the observed SOC in this system is a finite size effect [8]. However, it was claimed that a stretched exponential distribution for the avalanches fits the whole range of system sizes [9]. The reasons for not observing scaling are the existence of two angles of repose as observed in [7] and also the effect of inertia of the sand mass while moving down during avalanches.

This effect was suppressed in an experiment with anisotropic rice grains which used a pile of rice between two vertical glass plates separated by a small gap [10]. Rice grains were slowly dropped on to the pile. Due to the anisotropy of grains, various packing configurations were observed. In the steady state, avalanches of moving

rice grains refreshed the surface repeatedly. SOC behaviour was observed for grains of large aspect ratio, but not for the less elongated grains [10].

2. Internal Avalanches in a Granular Medium

In all the studies discussed above the avalanches propagate on the surfaces of the sandpiles. However, there exists the possibility of creating avalanches in the interior of a granular material. In a granular material kept in a bin at rest, different grains support one another by mutually acting balanced forces. Now if a grain is removed, the grains which were supported by it become unstable and tend to move. Eventually the grains in the further neighbourhood also lose their stability. As a result an avalanche of grain displacements takes place, which results in the upward propagation of some void space. The activity stops when no more grains remain unstable. We call this avalanche as the *Internal Avalanche*.

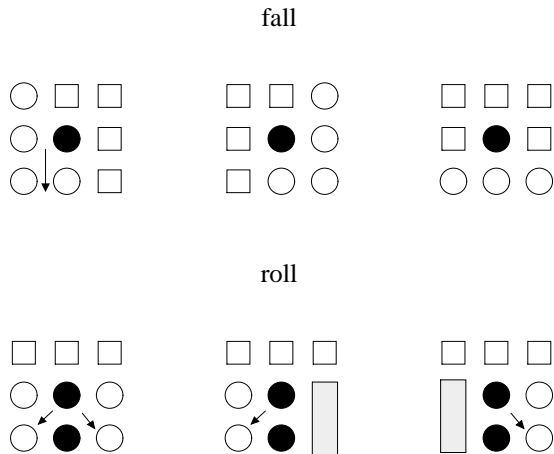


FIG. 1. The possible *fall* and *roll* moves in the cellular automata model of the granular system on the square lattice. Filled circle denotes the position of a grain, unfilled circle denotes a vacant site. The grain moves to the vacant position irrespective of the occupation of the sites with square boxes. Shaded rectangle denotes a pair of sites, in which at least one is occupied.

Depending on the method of perturbing the system we consider two kinds of internal avalanches. In its first kind, a randomly selected grain at the bottom of the granular bin is removed. The other way of creating avalanches is to make a hole at the centre of the bin and allow some granular mass to flow out. This flow soon stops by the formation of an arch which clogs the hole. The arch is then broken by removing one of its grains. We call these as internal avalanches of the second kind.

We believe, the internal avalanches are better candi-

dates for observing SOC. Due to the high compactness of grains in the granular material in a bin, a grain never gets sufficient time to accelerate much and therefore the effect of inertia should be small. The basic physical behavior here is thus quite different from the avalanches on the surface of the pile because of the constraints to particle motion in the dense particle beds.

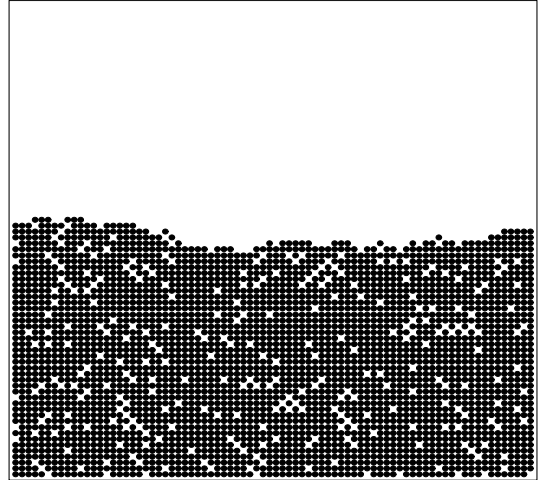


FIG. 2. The initial configuration grains in the Cellular Automata model. The bin of size 80×80 contains 2976 grains.

Internal avalanches were first studied in a two-dimensional semi-lattice model [11]. Non-overlapping unit square blocks model the grains, whose horizontal coordinates can vary continuously whereas the vertical coordinates are discretized. A grain can only fall vertically if insufficiently supported and sufficient space below is available. The system is disturbed by repeatedly removing grains one after another at the bottom of the bin and thus creating avalanches of grain movements. While this model and also other cellular automata [12] and ‘Tetris-like’ models [17] did exhibit scaling behaviour for the internal avalanches, the disc models [12,14,15] in continuous space, however, did not show sufficient evidence of SOC.

3. Cellular Automata Model

In the cellular automata model of a granular system an occupied (vacant) site on a lattice represents the presence (absence) of a grain [12]. A square lattice of size L with periodic boundary condition along the x axis represents the bin. The gravity acts in the $-y$ direction. The initial configuration of grains in the bin is generated by the ballistic deposition method. Grains are dropped along the randomly chosen vertical directions. After landing on the surface of the granular heap, the grain relaxes to its lowest energy position on the surface.

The different grain moves are explained in Fig. 1. A grain can have two types of possible moves in unit time: It can *fall* a lattice unit vertically, or it can *roll* either to the

lower left or to the lower right neighbouring positions. A single movement of a grain at $C(i, j)$ involves the neighbouring seven sites: $LU(i-1, j+1)$, $L(i-1, j)$, $LD(i-1, j-1)$, $D(i, j-1)$, $RD(i+1, j-1)$, $R(i+1, j)$ and $RU(i+1, j+1)$. In the *fall* move the grain comes down one level to the vacant site at D and in *roll* move the grain goes either to the vacant site at LD or at RD (Fig. 1). An arch is formed when a grain at C is considered stable if both of its two diagonally opposite sites either at LD and RU or, at LU and RD are occupied. As a result, on the square lattice, the only possible shape of an arch consists of two sides of a triangle. Initial granular patterns generated using the random ballistic deposition method with restructuring (BDRM) [16] and patterns are same for both models (Fig. 2). Depending on whether we allow the arch formations or not, we define the following two models.

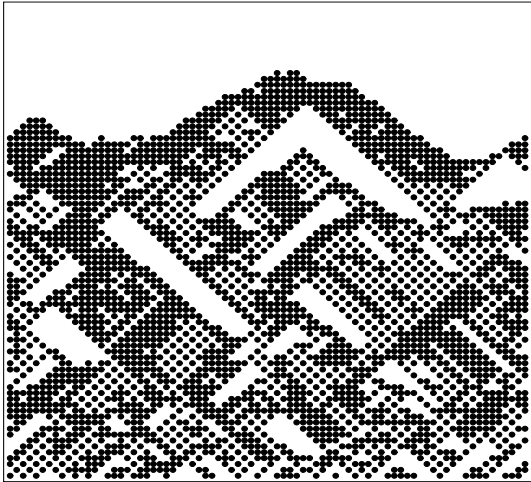


FIG. 3. A steady state granular pattern for the model A after a large number of avalanches starting from the initial pattern as in Fig. 2.

In model A we allow arch formations. The grain at C falls only if any of the following three conditions is satisfied: (i) LD , L and LU are vacant (ii) RD , R and RU are vacant (iii) LD and RD are vacant. In all other situations the grain does not fall. Notice that in conditions (i) and (ii) we are allowing the formation of arches. The grain at C rolls only if the site D is occupied. This is done in any of the three following ways: (i) If both LD , L are vacant but either of RD , R is occupied then the grain rolls to LD . (ii) if both RD , R are vacant but either of LD , L is occupied then the grain rolls to RD . (iii) If all four sites at LD , L , RD , R are vacant then the grain rolls either to LD or to RD with probability 1/2. A steady state pattern for the model A after a large number of avalanches is shown in Fig. 3.

In model B we do not allow arch formations. The first two conditions for fall of model A are modified as: (i) LD and L are vacant (ii) RD and R are vacant. All other

conditions of fall as well as roll remain same as in model A. A steady state pattern for the model B after a large number of avalanches is shown in Fig. 4.

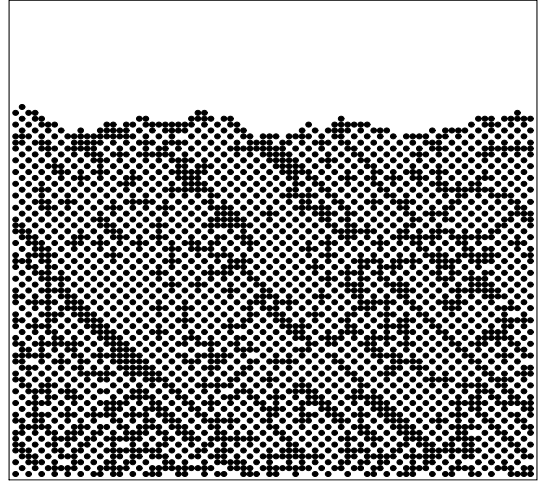


FIG. 4. A steady state granular pattern for the model B after a large number of avalanches starting from the initial pattern as in Fig. 2.

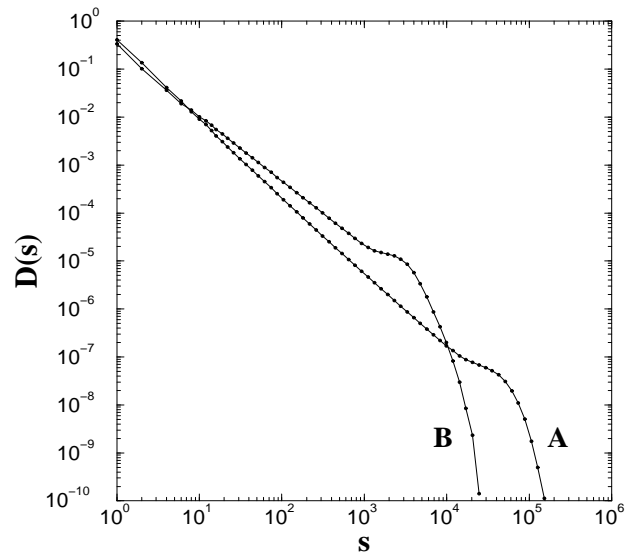


FIG. 5. The coarse grained distributions of avalanche sizes for the models A and B for system sizes 256×256 .

The avalanches are created by taking out one grain at a time at the bottom, allowing the system to relax and replacing it randomly on the surface after the avalanche is over. We see that the average density of sites, starting from an initial value of 0.907 ± 0.005 , decreases to the final stable value of 0.590 ± 0.005 in model A and to 0.618 ± 0.005 in model B. The avalanche size s and life time t follow power law distributions: $D(s) \sim s^{-\tau_s^A}$, $D(t) \sim t^{-\tau_t^A}$ and similarly for the model B (Fig. 5). Different exponents are obtained for the two

models: $\tau_s^A \approx 1.48$ and $\tau_t^A \approx 1.99$ where as $\tau_s^B \approx 1.34$ and $\tau_t^B \approx 1.50$.

4. The Tetris Model

The Tetris model is defined on an oriented (at 45° with the y axis) square lattice with periodic boundary condition along the x direction, gravity acts along the $-y$ axis [17–19]. The bottom is closed and grains are released at the top. The grains in this model are of asymmetric shapes. In the simplest version of the model, particles are represented by rectangular plaquettes of sizes $a \times b$. These grains are positioned at the lattice sites with two possible orientations i.e., the length of the grains can be aligned along any of the two principal axes of the lattice. The size of the grain is chosen in lattice units as: $a > 1/2$ and $a + b < 1$. Excluded volume effect is strictly maintained, that is overlapping of any two grains is just not allowed. An immediate consequence of this result is no two grains with their axes along the same principal axis can be positioned at the neighbouring lattice sites, however, they can position at neighbouring sites with their axes parallel.

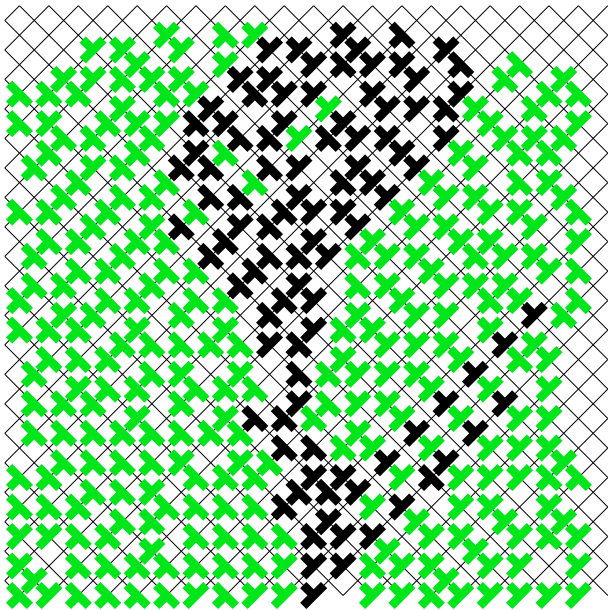


FIG. 6. A steady state configuration of the Tetris model where anisotropic grains have the shape of a T. Grains can have two different orientations. The boundary conditions are periodic in the horizontal direction. The black grains are disturbed in the avalanche caused by removing the lowest black grain.

The initial stack of grains in the bin of size $L_x \times L_y$ is generated by releasing grains one after the other at the top level of $y = L_y$. The orientation of a grain along either of the two lattice axes is randomly selected with equal probability. Grains retain their orientations as they

move and are not allowed to rotate. The grain then executes a directed random walk, at each step it makes a jump to one of the two downward neighbours which are along and perpendicular to its axis. It settles at a site from which it cannot come down further due to the excluded volume effect [18,19].

The granular system is then repeatedly driven by removing one grain at a time from the bottom. Each time a grain is removed, it makes the neighbouring grains unstable. This instability propagates upwards involving other grains in the system in the form of an internal avalanche until it gets arrested, when no further grains move and the system becomes stable again. The grain is the dropped again from the top to conserve grain number in the system.

The size of the avalanche is defined as the total number of grains destabilized by the process of removing a grain at the bottom. The size distribution of the avalanches follows a power law: $D(s) \sim s^{-\tau}$. Numerical simulations suggests a value for $\tau = 1.5 \pm 0.05$ [18,19].

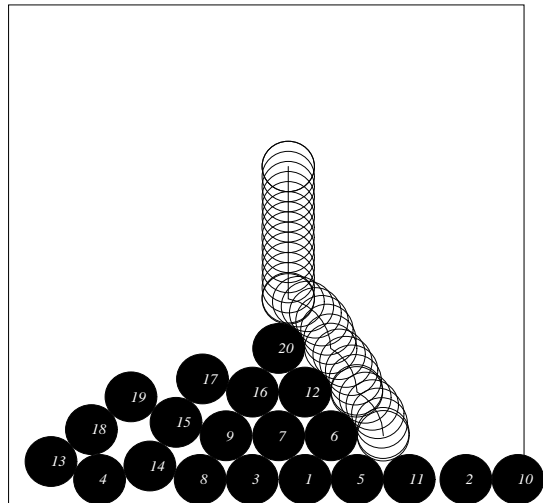


FIG. 7. Procedure for adding a single grain to the surface of a granular heap in a bin, using the Ballistic deposition by restructuring method. The already formed heap has 20 grains. The 21-st grain is being deposited in a sequence of successive ‘fall’ and ‘roll’ moves.

5. The Hard Disc Model

During the propagation of an avalanche in a granular medium grains compete locally with one another to occupy the same vacant space. The high packing densities of the grains in the bed prevent a single grain from occupying the available void space, and consequently grains get locked to form ‘arches’ [2]. A stable arch in a two dimensional granular pattern is a chain of grains where

the weight of each grain is balanced by the reaction forces from two neighbouring grains in the chain. Arches can form only when a grain is allowed to roll over other grains.

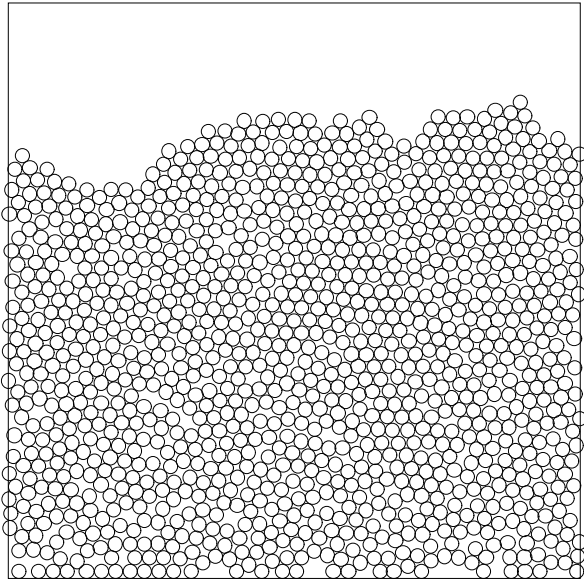


FIG. 8. A stable state configuration of the hard disc model after a large number of avalanches in a bin of size 80×80 containing 1200 grains.

The arch formations are very well reproduced if the grains are modeled as hard spheres. We study the two dimensional version of this system. The granular material is a collection of grains modeled by N hard mono-disperse discs of radii r . No two grains are allowed to overlap but can come very close to each other. In fact a grain can touch another grain and roll on it. The granular bin is represented by a rectangular area on the $x - y$ plane: from $x = 0$ to L_x and $y = 0$ to L_y . Periodic boundary condition is imposed along the x direction and gravity acts along the $-y$ direction. The bottom of the bin coinciding with $y = 0$ line is highly sticky and any grain which comes in its contact gets stuck there and does not move further.

The initial grain pattern is generated by the ‘ballistic deposition and restructuring method (BDRM)’ [16] (Fig. 7). In this method, grains are released at random positions at the top level of $y = L_y$ sequentially one after the other. Subsequently, they are allowed to fall vertically till they come in contact with the pile when they roll down to their stable positions along the paths of steepest descent. When all N grains are dropped, we have the initial configuration (Fig. 8).

Each grain is assigned a serial number n from 1 to N . The centre coordinates of these grains are stored in the $x_N(n)$ and $y_N(n)$ arrays. Very often we search the set of grains that reside in the local neighbourhood of a particular grain n . As a brute force solution one can

calculate the distances r_{nm} of the centres of all other grains ($m = 1, N; m \neq n$) from the centre of the n -th grain and pick up those grains which are within the local neighbourhood. This takes CPU proportional to N .

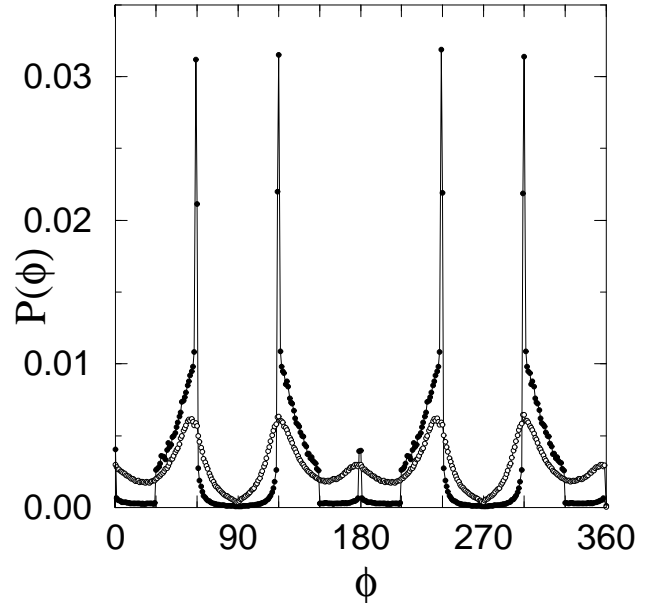


FIG. 9. Distribution $P(\phi)$ of the angles ϕ of the contact vectors. The plot for the initial distribution is shown by black dots. It has four high peaks at $60^\circ, 120^\circ, 240^\circ, 300^\circ$. The curve with opaque circles corresponds to the steady state. The randomness introduced into the system is reflected by the drastic reduction of the height of the peaks as well as a broadening.

The search is done more efficiently by considering an underlying grid S . A primitive cell is referred by the coordinates of its bottom-left corner (i, j) . If the centre of a grain n with coordinates (x_n, y_n) is within the primitive cell (i, j) then the location (i, j) in the S array is assigned the grain number n . A primitive cell can contain the centre of at most one grain if the radii of the grains are chosen as $r = 1/\sqrt{2} + \epsilon$, where ϵ is a small positive number. Therefore if the $S(i, j)$ location is zero, it implies that the cell (i, j) does not contain the centre of any grain.

The local neighbourhood LN of a grain whose centre is within the cell (i, j) by the area extending from $(x = i - 2$ to $x < i + 3$ and $y = j - 2$ to $y < j + 3)$. Only the grains, whose centres are within LN may overlap with the grain whose centre is within the cell (i, j) . While searching for the set of grains within LN , we search the lattice locations $i - 2$ to $i + 2$ and $j - 2$ to $j + 2$. Numbers stored in these locations give the grain numbers and their centre coordinates are obtained from the $x_N(n)$ and $y_N(n)$ arrays. This search takes CPU proportional to N^0 .

The temporal evolution of the granular system is studied by a ‘pseudo-dynamics’. Unlike the method of molecular dynamics we do not solve here the classical equations

of motion for the grain system. Only the direction of gravity and the local geometrical constrains due to the presence of other grains govern the movement of a grain. In our method a grain can have only two possible movements namely the un-obstructed vertical *fall* and the un-obstructed *roll* over another grain in contact. A parameter δ is introduced to characterize the fall and the roll moves. Time is discretized and in a unit time a grain may fall to a maximum height of δ or its centre can roll a maximum angle of $\theta = \delta/2r$ over another grain. During both fall and roll a grain does not accelerate. We believe this dynamics models an assembly of very light grains in 0+ gravity.

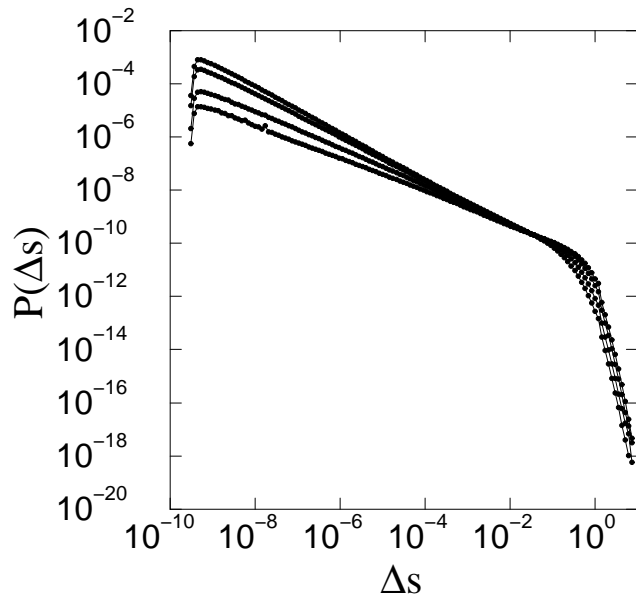


FIG. 10. Distribution $P(\Delta s)$ of the displacement Δs of the grains in a granular system. Curves for different sizes with grain numbers $N = 300, 625, 2500$ and 10000 are plotted from bottom to top on the left.

Since the grains are all of equal radii, a grain may be in contact with a maximum of six other grains. To recall quickly the set of grains in contact with an arbitrarily selected grain n we store the serial numbers of the contact grains for every grain into an array $neb(N, 6)$. The grain n may be at rest on two other grains and its weight is balanced by the reaction forces from them. The centres of the supporting grains must be on the two opposite sites of the vertical line passing through the centre of the stable grain n . We reserve the location $neb(n, 1)$ to store the serial number n_L of the left supporting grain and $neb(n, 2)$ to store the serial number n_R of the right supporting grain. The serial numbers of all other grains which are in contact with the grain n are kept one after the other in any order in the locations $neb(n, m)$, $m = 3, 6$.

To find out the neighbours in contact with a grain n we follow the following procedure. We first make a list of grains whose centres are within the local neighbour-

hood LN of the grain n . From this list, we sort out those grains whose centres are within a distance $2r - \epsilon_1$ to $2r + \epsilon_1$ from the centre of n , ϵ_1 being the tolerance factor which takes care of the accumulation of errors originated from real number manipulations. We consider these grains are in contact to the grain n . For each contact grain we calculate the angle ψ measured from the vertically downward direction through (x_n, y_n) to the vector starting from (x_n, y_n) to the centre of the contact grain. This angle ψ is measured +ve in the anti-clockwise direction and -ve in the clockwise direction. We first find out two contact grains with minimum values of ψ in the positive and the negative directions. If the sum of the magnitudes of these two angles is less than π , the grain n is considered at rest.

When a grain n is updated, it first selects the type of movement it is going to take:

- a. If $n_L = n_R = 0$ the grain n is allowed to fall.
- b. If $n_L \neq 0$ but $n_R = 0$ the grain n is allowed to roll on the right over the supporting grain n_L in contact at the left.
- c. If $n_L = 0$ but $n_R \neq 0$ the grain n is allowed to roll on the left over the supporting grain n_R in contact at the right.
- d. If $n_L \neq 0$ and $n_R \neq 0$ the grain n is considered a stable and does not move.

The *fall* movement of a grain n is executed in the following way. Corresponding to every grain in the local neighbourhood LN we first calculate the distance through which n should come down vertically to make a contact. The minimum δ_m of these distances corresponds to the grain t with the centre at (x_t, y_t) . If $\delta_m < \delta$ the grain n is brought down a distance δ_m so that it just touches t . The new coordinates are given by:

$$x'_n = x_n, \quad y'_n = y_t + \sqrt{4r^2 - (x_n - x_t)^2}.$$

However if $\delta_m \geq \delta$, the grain n falls a distance δ only. The neighbour lists of the grains n and t are updated. The lattice S is updated for the movement of the grain n and therefore the lattice point corresponding to (x_n, y_n) is vacated whereas that corresponding to (x'_n, y'_n) is occupied.

Now consider the situation when a grain n rolls over another grain t with the centre at (x_t, y_t) . The minimum angle θ_m through which the grain n should freely roll to be in touch with another grain m in the neighbourhood LN with the centre at (x_m, y_m) is calculated. If $\theta_m < \theta$ the grain n is rolled an angle θ_m over the grain t so that it simultaneously touches both the grains t and m . The centre coordinates (x'_n, y'_n) of the grain n in the new position are given by:

$$x'_n = \frac{1}{2}(x_m + x_t) \pm (y_m - y_t) \sqrt{\frac{4r^2}{d_{mt}^2} - \frac{1}{4}}$$

$$y'_n = \frac{1}{2}(y_m + y_t) \mp (x_m - x_t) \sqrt{\frac{4r^2}{d_{mt}^2} - \frac{1}{4}}$$

where d_{mt} is the distance between the centres of the grains m and t . If the angle $\theta_m \geq \theta$, the grain n rolls an angle θ over the grain t . In both cases if it happens that $y'_n < y_n$, then the grain n is brought at the same level as the grain t and $x'_n = x_n \pm 2r$ and $y'_n = y_n$ are assigned. The lattice S is renewed for the movement of the grain n and therefore the lattice point corresponding to (x_n, y_n) is vacated whereas that corresponding to (x'_n, y'_n) is occupied. The \pm signs are for the left and right rolls. The neighbour lists of the grains n and t are also updated.

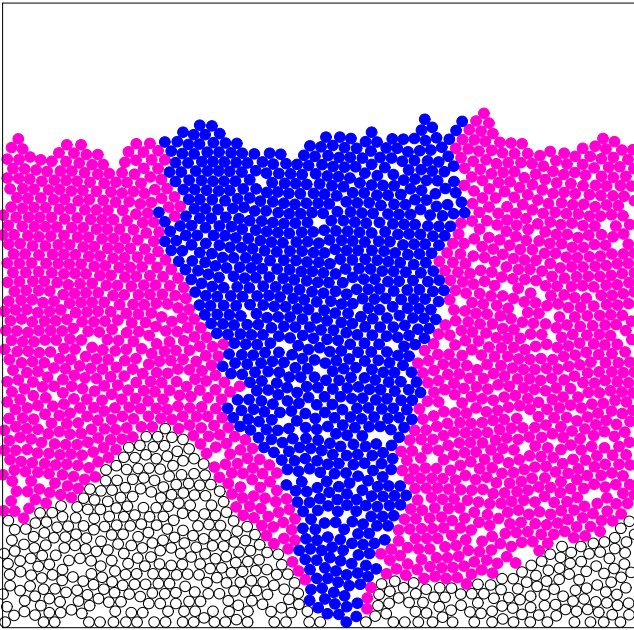


FIG. 11. The steady state configuration for a system of 2500 grains in a bin of $L_x = 80$. The gray and the black circles denote the grains in the supporting cluster of the lower most circle at the bottom. If this circle is deleted, only the black circles will move, which constitute the avalanche cluster. The vacant circles are the undisturbed grains.

5.1. Internal Avalanches of the First Kind

The system of N grains resting in the bin are disturbed by removing an arbitrary grain n at the bottom of the bin. A list of the discs residing at the bottom is made. To create an avalanche, a member of the list is randomly chosen and the corresponding disc at the bottom is deleted at time $t=0$. A number of neighbouring grains depend on the grain n for their stability. These grains will be unstable and start to move and so also

their further neighbours. A grain n is updated by checking its first two locations in the neb array i.e., $neb(n,1)$ and $neb(n,2)$ and determine which type of movement it is going to execute. In general, at any time t we have a list of unstable grains. When we update them some become stable but others remain unstable. The new list at time $t+1$ consists of these unstable discs from time t in addition to the neighbouring grains which become unstable due to motion of grains in time t . The avalanche of grain displacement stops when the list is empty. In a certain time t the grains are updated sequentially. After the avalanche stops, the removed grain is kept back at the surface of the pile by releasing again at an arbitrary position at the top level.

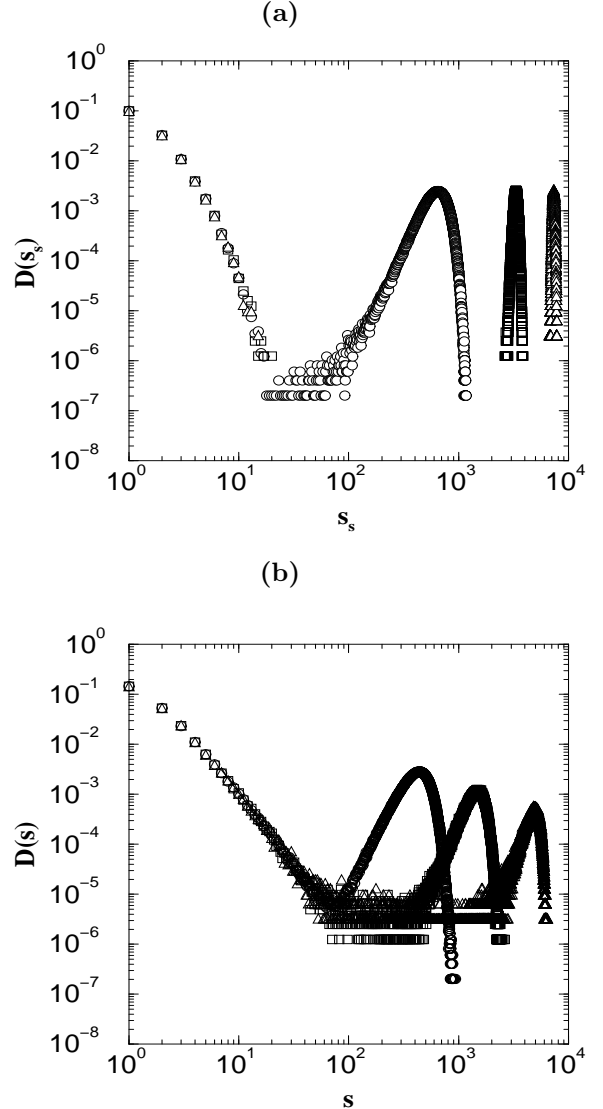


FIG. 12. (a) Distributions of the supporting clusters (s_s) for the systems of 2000 (circle), 4000 (square) and 8000 (triangle) grains. For small values of s_s , all curves fall on one another. The humps at large sizes shift linearly with the average height of the heap. (b) Distributions of the sizes of the avalanche clusters (s) for the same systems as in top figure.

The steady state of the system is characterised in two ways. The average area coverage over the whole granular system in the bin decreases with time (here time is measured by the number of avalanches) and finally reaches a steady value of 0.748 ± 0.005 . A similar study but with different initial configurations with a different value of average initial area coverage shows that in the final steady state area coverage reaches the same value. This implies that the final stable state is independent of the initial state which is a requirement of Self-Organized Criticality.

However, the area coverage has a local variation also and in the steady state it is found to vary with the vertical height, the granular pattern becoming denser with increasing height. Most of the arches reside at the bottom creating more vacant regions at the bottom. There are many avalanches which do not reach the surface, therefore in the upper part of the pattern not many arches are formed and packing is more compact. We expect that the area coverage should grow to a maximum value of 0.8180 ± 0.0002 near the top of the pile as quoted in [16] for the initial configuration at $t = 0$.

The steady state may also be characterised by the distribution of the angles of the contact vectors. When two grains are in contact, we draw two vectors from their centres to the contact points. The angle ϕ is the angle between the contact vector and the $+x$ direction. We measured the probability distributions $P(\phi)$ in the range $0^\circ - 360^\circ$ for the initial state as well as in the steady state. To arrive at the steady state we discard $2N$ avalanches, though the steady state attains even earlier than that.

The contact angle distributions are shown in Fig. 9. The plot of $P(\phi)$ vs. ϕ for the initial grain distribution shows four sharp peaks at $60^\circ, 120^\circ, 240^\circ, 300^\circ$. We explain them in the following way. If the grains were placed at the bottom in a complete orderly way by mutually touching one another without any gap, the structure generated by the BDRM method would be the hexagonal close packing (HCP) structure where every grain has six other grains in contact at the interval of 60° s. However, in our case, though we dropped grains randomly at the bottom level, the deterministic piling process retains some effect of the HCP structure. On the other hand, it is also known that the probability of a grain having the number of contact neighbours different from four, decreases with the height as a power law [16], which is certainly consistent with the four peaks we obtained. There are also two small peaks at 0° and at 180° due to the horizontal contacts of grains near the base level. This distribution, however, changes drastically by reducing the heights of the peaks and by broadening their widths in the steady state. The randomness introduced into the system by randomly selecting grains at the bottom increases the possibilities of other contact angles also, but is not fully capable to totally randomize it to a flat distribution. We check that after a large number of avalanches,

this steady state distribution remains unchanged.

How big are the displacements of the individual grains taking part in the avalanche? The displacement Δs is the absolute magnitude of the displacement of a grain before and after an avalanche. We observe that there is a huge variation the displacements Δs of the grains. Most of the grains displace very little, whereas others have much bigger displacements, but their numbers are small. The displacement distribution $P(\Delta s)$ is measured in the steady state over a large number of avalanches. The lower cut-off of the distribution turned out to be strongly dependent on the tolerance factor ϵ_1 used for the simulation. The upper cut-off of the distribution is of the order of unity since when a grain is deleted at the bottom, its neighbouring grains drops a distance of the order of the grain diameter.

Systems of four different sizes have been simulated with $N = 300, 625, 2500$ and 10000 in bins with base sizes $L_x = 20, 40, 80$ and 160 units respectively. First $5N$ avalanches are thrown away to allow the system to reach the steady state. A list is maintained for the coordinates of all grains. This list is compared before and after the avalanche to measure Δs . We observe a nice straight line curve over many decades of the $P(\Delta s)$ vs. Δs plot on a double logarithmic scale, with little curvature at the right edge implying a power law distribution for the displacement distribution (Fig. 10). However, the slope of this curve is found to increase with the system size and on extrapolating the slopes with $L^{-1/2}$ we obtain the asymptotic slope ($N \rightarrow \infty$ limit) to be 0.97 ± 0.05 . We get similar behaviours for the distributions of the x and y components of the displacement vectors as well.

In a stable configuration, the grains residing at the bottom supports the weights of the grains above. A grain at the bottom supports the partial weights of the few other neighbouring contact grains residing above it. These neighbouring grains also supports further neighbouring grains. Therefore, each grain at the bottom supports a large number of grains above it. We call the set of supporting grains as the ‘supporting cluster’ corresponding to the grain at the bottom (Fig. 11).

We measure the size of the supporting cluster s_s as the number of supported grains. While creating an avalanche, we randomly select a grain at the bottom. Before deleting it, we calculate the value of (s_s) . The supporting cluster distribution is plotted using a double logarithmic scale in Fig. 12(a) for three system sizes of $2000, 4000$ and 8000 grains contained within a bin of size $L_x = 100$. We see that each plot is having two distinctly separate regions. For small values of s_s we see a sharply decreasing variation, far from being a power law. For large values of s_s we see a peaked variation. We explain, that in most cases, the supporting cluster reaches the surface of the heap. However, in some cases, the supporting cluster is completely surrounded by an arch and therefore the cluster cannot be extended to the

surface. Since in the steady state, the arches are not of all length scales, and has a characteristic size, the supporting clusters which do not reach the surface also has a characteristic size.

The avalanche cluster size s is measured by the total number of grains displaced in an avalanche in comparison with the initial configuration. A snapshot of the configuration showing the supporting cluster, avalanche cluster as well as the set of undisturbed grains are shown in Fig. 11. The avalanche cluster size distribution is also plotted using a double logarithmic scale in Fig. 12(b). For small values of s we get a value of the slope around 2.95. If we assume that the distribution is described by a power law for small s , as $D(s) \sim s^{-\tau}$, then $\tau = 2.95$.

Now we comment on the effect of the parameter δ . Since, during the avalanche, different grains are updated in a sequence, the final steady configuration depends on the sequence in which different grains were updated. In the limit of $\delta \rightarrow 0$, this dependence will vanish. We observe that, on decreasing δ , the avalanche cluster size increases and in the limit of $\delta \rightarrow 0$, the avalanche cluster and the supporting cluster should be the same.

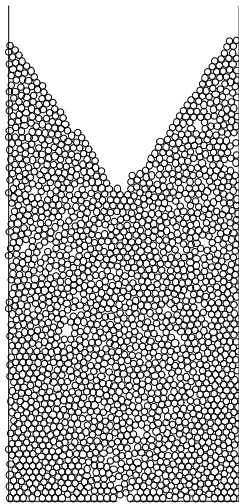


FIG. 13. A granular system of 2000 grains of radii $1/\sqrt{2}$ unit in a bin of width 50 units. The bin has a hole of width 3 units at the centre. The figure shows the steady state of the system after 3000 avalanches.

Therefore, we believe that the exponent $\tau=2.95$ is actually a result of the finite $\delta = r/10$ used in our simulation. If we reduce delta with the $D(s)$ vs. s plot should look alike as the $D(s_s)$ vs. s_s plot. To show that numerically, however, turned out to be difficult. We simulated a particular cluster in a system of $N = 2500, L_x = 80, s_s = 2068$, using $\delta, 10^{-1}\delta, 10^{-2}\delta$. The avalanche cluster sizes obtained are: 1046, 1080, 1081 respectively.

We conclude that, small avalanches, which do not reach the granular surface are unlikely to be of all sizes because the lengths of the arches present in the system in the stationary state are not of all sizes. Therefore an arbitrary

avalanche is most likely to reach the surface. However, the avalanche size has a distribution, which looks like a power law for finite δ but we expect that this behaviour is temporary and in the limit of $\delta \rightarrow 0$, the distribution should fall faster like that of the supporting cluster size distribution.

5.2. Internal Avalanches of the Second Kind

The flow of granular mass through a hole at the bottom of a granular bin is studied here. If the hole is sufficiently small, the outflow of grains stops soon due to the formation of a stable arch of grains clogging the hole. If the arch is broken, the grains in the arch become unstable and a cascade of grain displacements propagates within the system what we call as the Internal Avalanche of the second kind. As a result, a fresh flow starts through the hole, which also eventually stops due to the formation of another arch. It is known that the amount of out flowing granular mass between successive clogging events varies over a wide range, however, on average it depends sensitively on the hole diameter as compared to the grain size.

We study distribution of outflow sizes from a granular bin in two-dimensions and observe its power law variation [20].

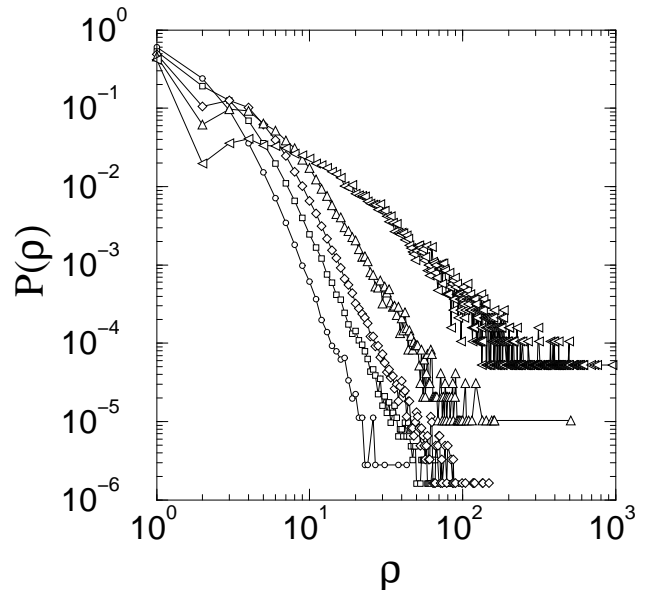


FIG. 14. The distribution $P(\rho)$ of the number of grains ρ that flows out of the system in an internal avalanche of the second kind between two successive clogged situations plotted on a double logarithmic scale. A bin of size $L_x = 50$, containing 4000 grains of radii $r = 1/\sqrt{2}$ was simulated with the hole sizes $R = 0.75, 1, 1.25, 1.5, \text{ and } 2.0$ (curves from left to right).

We study a two-dimensional granular system with grains kept in a vertical rectangular bin. Initially the system has no hole at the bottom and we fill the bin

up to a certain height. A hole of half-width R is then made at the centre of the bottom. Some grains drop out through the hole. This flow is stopped when an ‘arch’ is formed which covers the hole, forbids other grains to flow out and the system attains a stable state. The two lower most grains of the arch on the two sides of the hole are chosen and one of them is selected randomly. By deleting this grain, the arch is made unstable, which creates an internal avalanche of grain movements within the bin. Grains which come down and touch the bottom line of the bin with their centres within the hole are removed. While removing such a grain, the whole avalanche dynamics is frozen and the grain is replaced back on the top surface again by the BDRM method. A granular pattern after a large number of avalanches of second kind is shown in Fig. 13.

We count the number of grains ρ that flow out of the system during an avalanche between two successive clogging events and study its distributions for various values of the hole sizes R . We used a bin of dimensions $L_x = 50$ and $L_y = 200$ units containing 4000 grains of radii $r = 1/\sqrt{2}$.

In the steady state, two conical shapes are formed. The grains which are never disturbed by any avalanche are located on both sides of the hole. These undisturbed grains form a cone. The second cone is formed on the upper surface, though the grains were dropped on this surface along randomly chosen horizontal coordinates with uniform probability. For a fixed size of the base, the angle of the cone is found to increase with the average height of the granular column.

Holes of five different sizes, i.e., $R = 0.75, 1, 1.25, 1.5, 2$ are used. We could generate around 5×10^5 such outflows for each hole size and collected the distribution data for $P(\rho)$. We show the plot of these curves in Fig. 14 on a double logarithmic scale. The grain which is deleted to break the arch is also counted in ρ . It is found increasingly improbable that the outflow will consist of only another grain. Consequently $P(1)$ is found to decrease monotonically on increasing R . However, for large values of ρ , $P(\rho)$ decays.

All curves of $P(\rho)$ vs. ρ plots show straight lines for large ρ values, signifying the power law distributions for the avalanche sizes. The slopes of these curves $\sigma(R)$ are found to depend strongly on the size of the hole, as well as the grain size: $P(\rho) \sim \rho^{-\sigma(R,r)}$. We observe that $\sigma(R,r)$ is actually a linear function of (R/r) as $\sigma(R,r) = a - k(\frac{R}{r})$ with $k=1.6$. The average outflow $\langle \rho(R/r) \rangle$ diverges exponentially as: $\exp(\alpha(\frac{R}{r} - 1))$ with $\alpha = 0.7$.

Financial support by the Indo-French Centre for the Promotion of Advanced Research (IFCPAR) through the project No. 1508-3 is gratefully acknowledged. I also thank my collaborators in this project: Hans. J. Her-

rmann, Devang V. Khakhar, Stephane Roux and Supriya Krishnamurthy.

Electronic Address: manna@fermion.bose.res.in

-
- [1] A. Hansen and D. Bideau (eds.) *Disorder and Granular Media* (North Holland, Amsterdam, 1992).
 - [2] *Physics of Dry Granular Media*, Eds. H. J. Herrmann *et al*, Kluwer Academic Publishers, Netherlands (1998); A. Mehta *Granular Matter* (Springer, Heidelberg, 1994)
 - [3] C. Coulomb, *Memoires de Mathematiques et de Physique Presentes a l'Academie Royale des Sciences par Divers Savans et Lus dans les Assemblees* (L'imprimerie Royale, Paris, 1773) p. 343
 - [4] P. Bak, C. Tang and K. Wiesenfeld, *Phys. Rev. Lett.* **59**, 381 (1987); *Phys. Rev. A* **38**, 364 (1988).
 - [5] D. Dhar, *Physica A* **263**, 4 (1999); P. Grassberger and S. S. Manna, *J. Phys. (France)* **51**, 1077 (1990); S. S. Manna, *J. Phys. A* **24**, L363 (1992).
 - [6] P. Bak, *How Nature Works: The Science of Self-Organized Criticality*, (Copernicus, New York, 1996), H. J. Jensen, *Self-Organized Criticality*, (Cambridge university Press, 1998). D. Dhar, *Physica A* **263**, 4 (1999).
 - [7] H. M. Jaeger, C-h Liu and S. R. Nagel, *Phys. Rev. Lett.* **62**, 40 (1989).
 - [8] G. A. Held, D. H. Solina II, D. T. Keane, W. J. Haag, P. M. Horn and G. Grinstein, *Phys. Rev. Lett.* **65**, 1120 (1990).
 - [9] J. Feder, *Fractals* **3**, 431 (1995).
 - [10] V. Frette, K. Christensen, A. Malte-Sorensen, J. Feder, T. Josang and P. Meakin, *Nature (London)* **379**, 49 (1996).
 - [11] R. E. Snyder and R. C. Ball, *Phys. Rev. E* **49**, 104 (1994).
 - [12] S. S. Manna and D. V. Khakhar, *Phys. Rev. E.* **58**, R6935 (1998).
 - [13] S. Krishnamurthy, V. Loreto, H. J. Herrmann, S. S. Manna and S. Roux, preprint, 1998 *cond-mat* 9812074.
 - [14] S. S. Manna and D. V. Khakhar, in *Nonlinear Phenomena in Material Science III*, G. Ananthakrishna, L. P. Kubin and G. Martin (Eds.) (Transtech, Switzerland, 1995).
 - [15] S. S. Manna, *Physica A* **270**, 105 (1999).
 - [16] R. Jullien, P. Meakin and A. Pavlovitch, in *Disorder and Granular Media*, D. Bideu and A. Hansen (Eds.) (Elsevier 1993).
 - [17] E. Caglioti, V. Loreto, H.J. Herrmann and M. Nicodemi, *Phys. Rev. Lett.* **79**, 1575 (1997).
 - [18] S. Krishnamurthy, V. Loreto, H. J. Herrmann, S. S. Manna and S. Roux, *Phys. Rev. Lett.* **83**, 304 (1999).
 - [19] S. Krishnamurthy, V. Loreto and S. Roux *Phys. Rev. Lett.* **84**, 1039 (2000).
 - [20] S. S. Manna and H. J. Herrmann, *Eur. Phys. J. E* **1**, 341 (2000).